Z_2 Abelian Higgs: a cluster expansion approach

1987 J. Phys. A: Math. Gen. 20 2615

(http://iopscience.iop.org/0305-4470/20/9/043)

J. Phys. A: Math. Gen. **20** (1987) 2615-2628. Printed in the UK

Z_2 Abelian Higgs: a cluster expansion approach

M J Lamont

Department of Applied Mathematics and Theoretical Physics, University of Liverpool, PO Box 147, Liverpool L69 3BX, UK

Received 14 July 1986, in final form 28 October 1986

Abstract. The Z_2 lattice Abelian Higgs model in $D = 2 + 1$ is studied. New cluster expansion techniques which involve consideration of two perturbative terms are developed. These are used to obtain strong coupling expansions for the vacuum energy density and the mass gaps of both 'meson' and 'plaquette' excitations. The expansions are used, via Padé approximant techniques and duality considerations, to explore the phase diagram of the theory.

The location of the second-order phase boundaries are in good agreement with those obtained by other methods. The behaviour of the line of first-order transitions is examined and is estimated to terminate at $\lambda \geqslant 4.5$.

1. Introduction

Cluster expansion techniques have been applied with some success in obtaining strong coupling expansions of pure gauge theories via Hamiltonian formulations. An obvious extension of these methods is the consideration of Hamiltonians which contain matter fields as well as gauge fields. Eventually one would like to consider a realistic model—SU(3) gauge theory coupled to fermions—it being possible to treat fermions naturally in a Hamiltonian formulation (see, for example, Susskind 1977, Banks *et al* 1977). However in order to develop the techniques, a convenient candidate for consideration is the Z_2 Abelian Higgs model.

The model has an interesting phase structure which has been studied using a variety of methods (Banks and Sinclair 1981, Kogut 1980, Horn and Yankielowicz 1979, Horn and Katznelson 1980), and is discussed in some detail by Fradkin and Shenker (1979). The phase diagram is known to have three phases present. When the gauge field and matter field temperatures are low, a 'free charge' phase can exist. Here one has Coulomb-like interactions with massless gauge bosons. This phase is separated from a Higgs/confinement phase by second-order phase boundaries. In this other phase, one finds either massive Higgs bosons (short-range interactions due to charge screening, the vacuum expectation value of the matter fields being non-zero) or a confining phase (due to long-range gauge excitations). These two regions are separated by a line of first-order transitions which is thought to extend into, but terminate in, the region of confinement. The two phases have, in fact, been shown to be analytically connected (Fradkin and Shenker 1979) and thus, in effect, constitute a single phase.

In $D = 2 + 1$, strong coupling expansions for the theory have been obtained to low order (Banks and Sinclair 1981), using the standard Rayleigh-Schrödinger perturbation expansion. At higher orders, with the complication of two perturbative terms, this formulation becomes unmanageable. In this paper, cluster expansion techniques are

0305-4470/87/092615+14$02.50

used to obtain perturbative expansions in the strong coupling region for the vacuum energy density (VED) to x^{10}, and for the mass gaps of both the 'meson' and the 'plaquette' to x^8. A disagreement with earlier work is noted. The new expansions, along with the use of duality transformations, are used to explore the phase diagrams of the theory.

The mass gap vanishes at the second-order phase transition signalling the presence of massless excitations. The locations of these transitions are estimated using Padé approximants of the expansions. The first-order phase transition is investigated by calculating the latent heat on crossing the self-dual line in a suitable formulation of the theory.

The layout of the rest of the paper is as follows. In § 2 the formulation of the theory and the cluster techniques used are discussed. In § 3 the results and their analysis are presented. Section 4 contains conclusions on the results obtained and on the viability of the methods introduced in this paper.

2. Formulation and method

2.1. The Hamiltonian

The Hamiltonian under consideration is

$$W = -\lambda/\sqrt{\mu} \sum_l (\sigma_l) - \sqrt{\mu}/z \sum_s (\tau_l) - 1/\lambda\sqrt{\mu} \sum_p \sigma_3\sigma_3\sigma_3\sigma_3 - z\sqrt{\mu} \sum_l \tau_3\sigma_3\tau_3. \tag{2.1}$$

Here l labels links, s sites and p plaquettes. σ and τ are independent Pauli spin matrices, defined at the links and sites of a quadratic lattice, each with eigenvalues ± 1. By simple rescaling and change of variable one obtains the more convenient form

$$H = \sqrt{\mu}/2\lambda W = -\tfrac{1}{2}\sum_l (\sigma_1 - 1) - \tfrac{1}{2}\eta \sum_s (\tau_1 - 1) - x \sum_p \sigma_3\sigma_3\sigma_3\sigma_3 - \xi x \sum_l \tau_3\sigma_3\tau_3 \tag{2.2}$$

where $x = 1/2\lambda^2$, $\xi = \mu\lambda z$ and $\eta = \mu/\lambda z$.

The Hamiltonian is invariant under local gauge transformations (Fradkin and Susskind 1978). The zeroth-order gauge invariant ground state has the eigenvalues of all σ_1 and τ_1 to be $+1$. Further gauge invariant states can be formed from closed paths of flipped links or from strings of links joining flipped sites. The lowest-lying gauge invariant excitations consist of either (i) a 'meson' excitation of flipped τ_1 on adjacent sites joined by a flipped σ_1, or (ii) a 'plaquette' of four flipped σ_1; which of these has the lowest energy will depend on the value of η.

The study of the model starts from the strong coupling region where x is small and ξ finite. The expansions derived here will thus be in x and ξx. In references below to order x^j, say, corresponding powers of ξ are implicit.

2.2. Cluster expansion techniques

The method used to produce the required expansions is a variation on the cluster expansion of Nickel (1980) and Marland (1981) which has been further developed and well documented by Irving and Hamer (1984a, b). The main complication here is the need to consider clusters which contain two 'species' corresponding to the possibilities of either 'plaquette' or 'meson' excitations. For example, connected clusters contributing to the VED to fourth order are shown in figure 1. Here a square

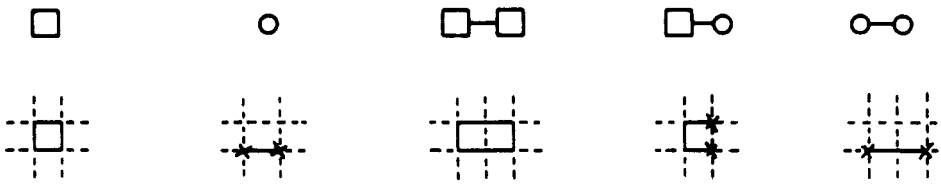

Figure 1. Connected clusters contributing to the VED up to x^4 and their lattice realisations.

represents a plaquette and an open circle a meson. The lattice realisations of these diagrams are also shown. In the calculation of the mass gaps, disconnected clusters must also be taken into consideration.

With pure gauge theories in $D=2+1$, a series for the VED to x^{2J} can be obtained using clusters of up to J plaquettes. However, with the introduction of Higgs fields, this is no longer true and one must consider clusters such as those shown in table 1. Here the clusters contribute at orders less than x^{2J}.

The VED per site for an infinite lattice may be expressed (see, for example, Irving and Hamer 1984b)

$$\lim_{N\to\infty}(\omega_0/N)=\sum l_{m,\alpha_m}\varepsilon_{m,\alpha_m} \tag{2.3}$$

where the sum runs over all linked clusters (m, α_m) made up of m points in configuration α_m. l_{m,α_m} is the lattice constant, i.e. the number of ways the cluster (m, α_m) can be embedded on the lattice, divided by the number of sites N. The quantities ε_{m,α_m} are the connected contributions made by the clusters (m, α_m) to the vacuum energy.

The ground-state energy for any given cluster (i, α_i) can be expressed as the sum of contributions from each embedded subcluster

$$\omega_0^{i,\alpha}=\sum C_{j,\alpha_j}^{i,\alpha_i}\varepsilon_{j,\alpha_j} \tag{2.4}$$

where the $C_{j,\alpha_j}^{i,\alpha_i}$ are the embedding constants for topologies (j, α_j) within (i, α_i). The aim here is to calculate the quantities ε_{m,α_m} as series expansions in two coupling constants by an iterative method, starting from small clusters (low order) and working upwards. To this end a variation on the expansion method used by Hornby and Barber

Table 1. Examples of J-point clusters contributing to order less than x^{2J}.

	J	Order
	5	ξ^4x^5
	6	ξ^6x^7
	8	ξ^6x^8

(1985), for use with two perturbative terms, was developed as described in appendix 1. Straightforward use of this algorithm for the VED enabled calculation of the $\omega_0^{i,\alpha}$. Inversion of (2.4) gives the ε, and subsequent summation yields the VED to requisite order.

A similar, albeit slightly more sophisticated, approach is required when considering the mass gaps. From standard perturbation theory it can be readily shown (Nickel 1980, Hamer and Irving 1985) that the mass gap F may be written

$$F = F_0 + \langle 1|V|1\rangle + \Delta \tag{2.5}$$

where F_0 is the unperturbed value of the mass gap and $|1\rangle$ is the unperturbed first excited state. Here $\langle 1|V|1\rangle$ makes no contribution and may be ignored. Δ may be written as an iterative perturbation expansion in the usual manner, expanding in powers of V:

$$\Delta = (\langle 1|V(P/F-H_0)V|1\rangle + \langle 1|V(P/F-H_0)V(P/F-H_0)V|1\rangle + \ldots)|_{\text{constant in } N}. \tag{2.6}$$

Here P is a projection operator onto states orthogonal to $|1\rangle$ and N is the number of sites in the system. Each term in the expansion may be represented by a connected or disconnected cluster. A cluster expansion for Δ may thus be written (Hamer and Irving 1985):

$$\Delta = \sum l'_{m,\beta_m} \varepsilon'_{m,\beta_m} \tag{2.7}$$

for the infinite lattice, and

$$\Delta_{n,\beta_n} = \sum C^{n,\beta_n}_{m,\beta_m} \varepsilon'_{m,\beta_m} \tag{2.8}$$

for a cluster. (m, β_m) denotes a set of m sites arranged in a topology β_m, which may be connected or disconnected. ε'_{m,β_m} is the contribution from all diagrams which span that topology and Δ_{m,β_m} is the total contributions from all diagrams contained within (m, β_m). The $C^{n,\beta_n}_{m,\beta_m}$ are again the embedding constants for topologies (m, β_m) within (n, β_n). l'_{m,β_m} is the overall lattice constant.

The aim, once more, is to calculate Δ_{n,β_n} for a given cluster as a perturbation series to some given order. An algorithm for use with two coupling constants was developed (see appendix 2). Here one calculates the mass gap F, via summation of the ε, exact to a given order in x. This is then used iteratively in the calculation of the contributions to next highest order.

Clusters were generated enabling expansions to x^{10} for the VED and to x^8 for the mass gaps. 148 connected clusters were required for the former and 342 disconnected clusters for the latter.

Storing the representation of the clusters is not a problem. However, beyond x^{10}, the time required to evaluate the mass gap series becomes the limiting factor, the number of clusters increasing rapidly with each additional order. The calculation is complicated by the need to consider J-point clusters contributing to orders less than x^{2J} (see table 1), which also proliferate as one moves to higher order.

In obtaining the series η is held fixed, resulting in expansions in x and ξx. The results are thus directly comparable with those of Banks and Sinclair (1981) where η appears explicitly. As some disagreement was noted, the analytic calculation of the mass gap series to x^4, via the Rayleigh-Schrödinger perturbative expansion (see, for example, Kogut 1979), was repeated. Errors were revealed in the series presented by Banks and Sinclair. The corrected series were in agreement with the new cluster computations and are shown in table 2. Also shown, in tables 3 and 4, are sample series expansions for the plaquette mass gap ($\eta = 5$) and the VED ($\eta = 1$) respectively.

Table 2. Coefficients of the strong coupling expansions for $E_{\text{link}} - E_{\text{vac}}$ and $E_{\text{box}} - E_{\text{vac}}$. In each case the subscript ij labels the coefficient of $\xi^i x^i$.

$E_{\text{link}} - E_{\text{vac}}$	$l_{00} = 1 + 2\eta$
	$l_{20} = -\frac{1}{2}$
	$l_{22} = -12 + 14/(1+2\eta)$
	$l_{32} = 16 + 4/(1+2\eta) + 4/(1+2\eta)^2$
	$l_{40} = +\frac{3}{32}$
	$l_{42} = (88\eta^3 + 524\eta^2 + 762\eta + 229)/4(1+2\eta)^3(3+2\eta)$ $-(120\eta^3 + 660\eta^2 + 1050\eta + 375)/4(1+2\eta)^3(5+2\eta) + \frac{1}{2}(2\eta - 3) - \frac{91}{6}$
	$l_{44} = (576\eta^4 + 672\eta^3 + 252\eta^2 + 178\eta - 2)/(\eta + 1)(2\eta + 1)^3$
$E_{\text{box}} - E_{\text{vac}}$	$b_{00} = 4$
	$b_{20} = -\frac{3}{2}$
	$b_{22} = -8/(4\eta^2 - 1)$
	$b_{40} = +\frac{43}{96}$
	$b_{42} = (560\eta^3 - 56\eta^2 - 492\eta + 238)/(1+2\eta)^3(3+2\eta)(1-2\eta)^2$ $-(80\eta + 120)/(1+2\eta)^2(5+2\eta)$ $-(60\eta + 42)/(1+2\eta)^3 + 32/(1+2\eta)^2(1-2\eta)^2(3-2\eta) - 5/(5+2\eta)$ $+17/(3+2\eta) - 35/2(1+2\eta) - 11/2(1-2\eta)$
	$b_{44} = -(864\eta^4 - 896\eta^3 + 424\eta^2 + 32\eta + 8)/(\eta^2 - 1)(4\eta^2 - 1)^3$

3. Analysis and discussion

3.1. The second-order phase boundaries

Having obtained expansions in x and ξx for the mass gaps, ξ was held fixed, its value depending on the particular value of μ under consideration. The second-order phase boundaries were located by analysis of the Padé approximants of the resultant series in x. The real positive zeros of the [2, 4], [3, 4], [3, 5] and [4, 4] Padés gave an estimate of the critical points. A standard Padé analysis of the logarithmic derivative (Dlog) of the series was also performed. If one assumes that the mass gap behaves as $F \sim (x - x_c)^{\nu}$ near the critical point, the pole and its residue give an estimate of the critical point and index respectively.

In the analysis of the Dlog series the number of terms under consideration and the influence of nearby complex singularities meant that only the [2, 4] Padé was reliable. One can motivate consideration of this particular Padé by comparison with similar analysis of the longer pure gauge series (Hamer and Irving 1985) and by its agreement with the zeros obtained directly from the original series. However, the critical index, which was found to lie within $\simeq 9\%$ of the estimates obtained from a finite-lattice treatment (Hamer 1983) and the analysis of the pure gauge series, must be viewed with reservation.

Here it is convenient to convert back to the original variables and utilise the duality properties of W (see, for example, Fradkin and Susskind 1978), where reversal of the roles of the links and sites of the lattice leave the Hamiltonian invariant under the mappings

$$\lambda \to z \qquad z \to \lambda \qquad \mu \to 1/\mu.$$

When $\mu = 1$, the phase diagram is thus symmetric under the interchange of z and λ. Likewise, a diagram with a particular value of μ and one with its reciprocal value are similarly related. Figure 2 shows the estimates obtained for the second-order phase boundaries when $\mu = 1$. The results obtained from the Dlog analysis are plotted.

Table 3. Sample series for the plaquette mass gap ($\eta = 5$).

	Constant	$(\xi x)^2$	$(\xi x)^4$	$(\xi x)^6$	$(\xi x)^8$
Constant	4	$0.808\,080\,8081 \times 10^{-1}$	$-0.188\,416\,1480 \times 10^{-1}$	$-0.185\,342\,5511 \times 10^{-1}$	$-0.798\,876\,9148 \times 10^{-2}$
x	—	—	$0.731\,865\,9859 \times 10^{-1}$	$0.280\,848\,2904 \times 10^{-1}$	
x^2	$-\frac{3}{2}$	$-0.283\,892\,2123 \times 10^{-1}$	$-0.837\,909\,3558 \times 10^{-2}$	$-0.162\,291\,7386 \times 10^{-1}$	
x^3	—	—	$-0.449\,075\,4780 \times 10^{-1}$		
x^4	0.447 916 6667	$0.258\,948\,8758 \times 10^{-1}$	$0.797\,024\,5375 \times 10^{-2}$		
x^6	−0.723 126 4468	$-0.700\,829\,5909 \times 10^{-1}$			
x^8	$0.104\,078\,1117 \times 10^{+1}$				

Table 4. Sample series for the VED ($\eta = 1$).

	Constant	$(\xi x)^2$	$(\xi x)^4$	(ξx^6)	(ξx^8)	$(\xi x)^{10}$
Constant	0	−0.666 666 6667	−0.148 148 1481	$-0.679\,600\,2352 \times 10^{-1}$	$-0.184\,621\,5578 \times 10^{-1}$	$0.416\,469\,5346 \times 10^{-1}$
x	—	—	0.550 617 2840	0.483 731 1385	0.335 820 6968	
x^2	−0.25	$-0.777\,777\,7778 \times 10^{-1}$	−0.148 806 5844	$-0.136\,051\,0672 \times 10^{+1}$	$-0.185\,567\,0705 \times 10^{+1}$	
x^3	—	—	0.164 934 8422	0.694 261 4610		
x^4	$-0.520\,833\,3333 \times 10^{-2}$	$-0.939\,373\,8977 \times 10^{-2}$	$-0.523\,311\,6841 \times 10^{-1}$	−0.769 470 6465		
x^5	—	—	$0.341\,471\,8795 \times 10^{-1}$			
x^6	$-0.325\,520\,83 \times 10^{-3}$	$-0.116\,360\,045 \times 10^{-2}$	$-0.126\,762\,0040 \times 10^{-1}$			
x^8	$0.102\,290\,40 \times 10^{-3}$	$-0.340\,005\,30 \times 10^{-3}$				
x^{10}	$-0.108\,9566 \times 10^{-4}$					

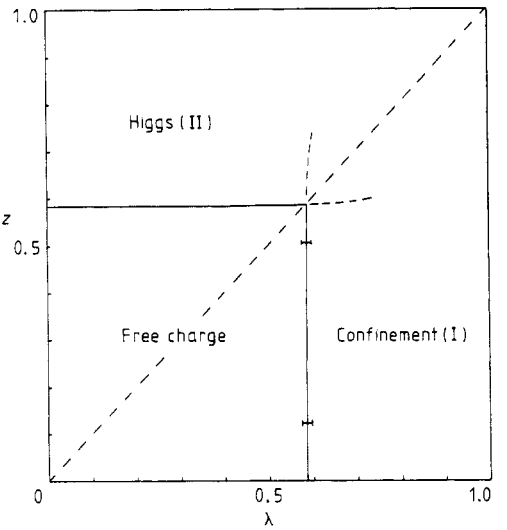

Figure 2. The phase diagram for $\mu = 1.0$. The full lines are the estimated positions of the second-order phase boundaries. Sample errors are estimated from the spread of the zeros.

Along the axes the theory reduces to either:

(i) the Ising model ($\lambda = 0$), or

(ii) the pure Z_2 gauge theory ($z = 0$).

The critical points of these theories are well established and the corresponding estimates obtained here agree well with, for example, the biased estimate of Hamer and Irving (1985) in the pure gauge case and that of Marland (1981) for the Ising model. Hamer and Irving's estimates were obtained from the analysis of a strong coupling expansion to x^{14} and thus give a measure of the accuracy of the results obtained here:

$$\lambda_c(x^8) \simeq 0.583 \qquad \text{pure gauge}$$

$$\lambda_c(x^{14}) \simeq 0.573 \qquad \text{pure gauge.}$$

These figures would suggest that the second-order phase boundaries shown in figure 2 would be shifted to lower $\lambda(z)$ by higher-order corrections. Comparison of these two values gives a good indication of the accuracy of the analysis, which is seen to be a considerable improvement on that obtained by Banks and Sinclair (1981) who obtained $\lambda_c = z_c \simeq 0.37$. The zeros corresponding to this value were obtained at low order in the Padé analysis. However, a study of the Padé tables shows it to be an unstable zero and in marked disagreement with values obtained here and elsewhere†.

From figure 2, it can be seen that the second-order phase transition continues into the diagram, showing remarkable consistency on approaching the self-dual line. There is little evidence for the marked curvature obtained by a $1/N$ expansion analysis (Kogut 1980). Estimates of the critical index were found to remain constant at $\nu \sim 0.59$,

† There seems to be some confusion in the literature as to the interpretation of the results quoted by Pfeuty and Elliott (1971). Careful reconsideration of the Hamiltonian used by the above led to the conclusion that the value quoted by Banks and Sinclair (1981) and Kogut (1980) should have been $\lambda_c = 0.570$ rather than $\lambda_c = 0.403$.

showing little change as one progresses into the phase diagram. This is in contrast to the results from one finite lattice study (Irving and Thomas 1982), but in agreement with the trends reported in another (Horn and Karliner 1982) and is also what one would expect from universality arguments. The point at which the second-order lines combine is estimated to be at $\lambda = z \simeq 0.59$.

Figure 3 shows the phase diagram with $\mu = 0.1$. The estimates obtained from $W(\lambda, z, \mu = 0.1)$ and $W(z, \lambda, \mu = 10)$ are plotted.

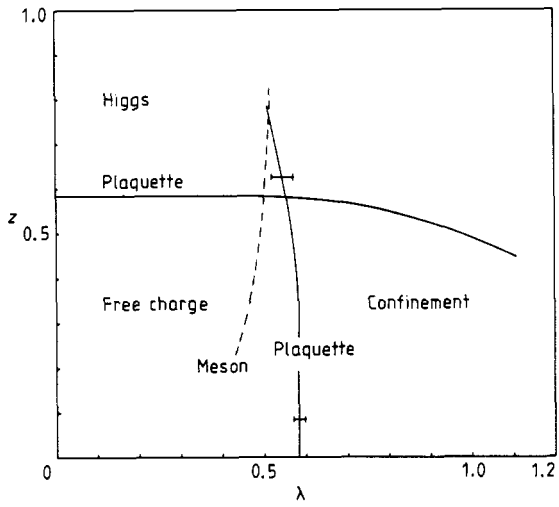

Figure 3. The phase diagram for $\mu = 0.1$. The full and broken curves show the positions of the second-order phase boundaries estimated from the plaquette and meson mass gap series respectively.

The phase transition between 'confinement' and 'free charge' occurs when the mass of the lowest-lying excited state goes to zero. In the unperturbed situation one would expect the 'meson' to take over from the 'plaquette' as the lowest-lying state at $\eta = \frac{3}{2}$. However the masses are 'renormalised' by perturbative effects which serve to pull the 'plaquette' mass below that of the 'meson' until η reaches some lower value (or vice versa depending on μ).

Thus for $\mu = 0.1$, the line of phase transitions for the 'meson' mass gap does not in fact represent the phase boundary, as supposed by Banks and Sinclair (1981), rather the much more satisfactory 'plaquette' line. For comparison both are plotted in figure 3. Comparison of figures 2 and 3 would suggest that the phase structure of the theory is insensitive to the value of μ.

3.2. The first-order phase boundary

The first-order phase transition between the Higgs(I) and the confinement(II) regions was investigated by considering the latent heat on crossing the self-dual line, $\lambda = z$ when $\mu = 1$.

The VED series in ξ, x may be re-expressed in terms of λ, z. The first few terms are

$$\text{VED}(z, \lambda) = -(2\lambda + 1/z) - 1/8\lambda^3 - z^3/(z\lambda + 2) + \ldots . \tag{3.1}$$

In terms of the symmetrical variables

$$\rho = \tfrac{1}{2}(z+\lambda) \qquad \tau = \tfrac{1}{2}(z-\lambda)$$

the self-dual line becomes $\tau = 0$ and the latent heat is given by

$$\Delta(\rho) = \tfrac{1}{2}\partial/\partial\tau(E_{\mathrm{I}} - E_{\mathrm{II}})|_{\tau=0}. \tag{3.2}$$

Now in practice by fixing η and ξ one is effectively considering the VED on a hyperbola $z\lambda = \xi$ in the z-λ plane (see figure 4). One is thus able to express the series in terms of z or λ alone. Calculation of Δ may thus be effected as follows:

$$\begin{aligned}\Delta &= \tfrac{1}{2}\partial/\partial\tau(E_{\mathrm{I}}(\lambda) - E_{\mathrm{II}}(z))|_{\tau=0} \\ &= \tfrac{1}{2}(\partial\lambda/\partial\tau\ \partial/\partial\lambda\ E_{\mathrm{I}}(\lambda) - \partial z/\partial\tau\ \partial/\partial\lambda\ E_{\mathrm{II}}(z))|_{\lambda=z=\sqrt{\xi}} \\ &= -\partial/\partial\lambda\ E_{\mathrm{I}}(\lambda)|_{\lambda=\sqrt{\xi}}.\end{aligned} \tag{3.3}$$

One can therefore Padé the derivative of the VED $\partial E_{\mathrm{I}}/\partial\lambda$ from the strong-coupling region (λ large) to the self-dual line, where the latent heat may be evaluated. The series for the VED was obtained for a wide range of η up to order λ^{-19} and the latent heat calculated as described above. The results obtained are shown in figure 5, where values from the [4, 4], [5, 5] and [6, 4] Padés are plotted. One can see that the results from the different Padé are consistent even at large λ (small η) which is well away from the strong-coupling regime. This would suggest that the number of terms in the series is sufficient for reasonable conclusions to be made. One would expect the latent heat and thus the line of first-order transitions to go to zero continuously, i.e. terminate in a second-order phase transition. This behaviour is seen to occur at low λ, the latent heat dropping smoothly to zero at $\lambda \sim 0.6$ which coincides very nicely with the junction of the two second-order phase boundaries.

At higher λ, one witnesses a smooth fall, figure 5 suggesting a drop to zero in the latent heat at $\lambda_c \geqslant 4.5$. Here the latent heat is small, and comparison of the [4, 4] and [5, 5] Padé values suggest that the effect of higher-order terms is to pull the latent heat down. How much so is open to question and consequently one is unable to make a

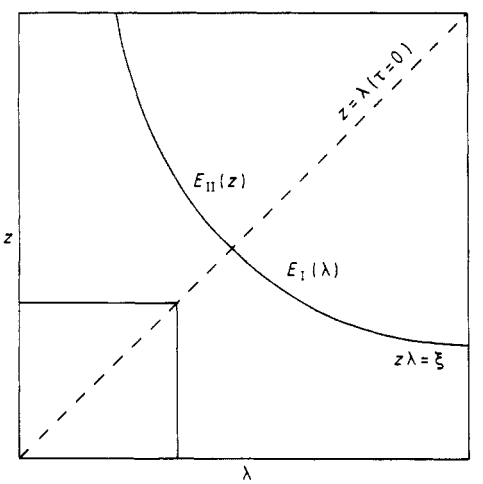

Figure 4. Diagram showing hyperbola and self-dual line used in calculation of the latent heat.

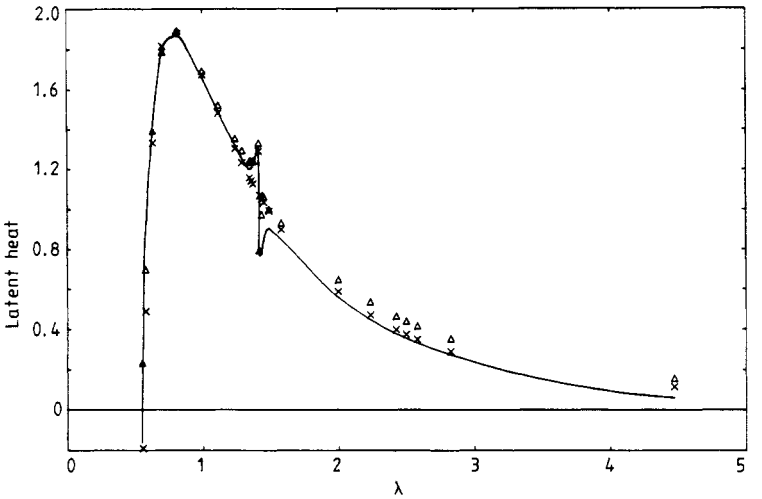

Figure 5. Variation of latent heat on crossing self-dual line against λ. Plotted are the [5, 5] (full curve), [4, 4] (△) and [6, 4] (×) Padé values.

particularly accurate estimate of λ_c, but the general trend is clear. A more precise location of the critical point would require a longer series expansion.

The estimate of λ_c obtained here is to be compared with the values $\lambda_c = z_c = 1.37 \pm 0.05$ and $\lambda_c = z_c \simeq 1.58$ found by a finite lattice study (Irving and Thomas 1982) and by the low-order $1/N$ expansion (Kogut 1980) respectively.

The conclusion that λ_c lies $\geqslant 4.5$ must be tempered by consideration of the curious feature apparent at $\lambda \sim 1.41$ ($\eta \sim 0.5$). The possibility of spurious poles in the Padés was considered. Standard quadratic Padés of the latent heat series were also performed and these also showed similar behaviour and so rule out this possibility. One is encouraged to regard the feature as a genuine effect due to the fact that it coincides with similar behaviour in the curvature of the β function in the finite lattice study (Irving and Thomas 1982) mentioned above. In this case it was identified, apparently without any very good reasons, as signalling the termination of the first-order line, the critical value being that quoted above.

Accepting the anomaly as a real feature, then either it is indicative of the expected critical point and the latent heat observed beyond this point is pulled to zero by higher-order corrections; or it reflects additional, as yet unrevealed, structure of the model, such as the presence of a metastability of some sort. This, however, remains an open question.

4. Summary and conclusions

New cluster expansion techniques have been used to derive series to order x^{10} for the VED and to x^8 for the mass gaps of the Z_2 Abelian Higgs model which extend those previously available. At low order, disagreement with results obtained elsewhere (Banks and Sinclair 1981) was noted and corrected expressions (to x^4) presented.

Analysis of the mass gap series, which although not particularly well behaved, enabled the second-order phase boundaries to be located with some confidence. The results were in good agreement with those obtained elsewhere (Horn and Karliner

1982, Irving and Thomas 1982) and a marked improvement on those obtained by analysis of a low-order strong coupling expansion (Banks and Sinclair 1981). The critical index was found to be constant as one moves along the second-order transition line, at variance with a finite lattice study (Irving and Thomas 1982), but in agreement with another (Horn and Karliner 1982) and with what one would expect from universality considerations.

The increased length of the series obtained meant that it was possible to investigate the first-order phase transition for the first time. The results suggest that the first-order line vanishes at higher λ than was previously suggested by a finite lattice study and a low-order $1/N$ calculation.

The motivation of the paper was to explore the viability of new cluster expansion techniques for obtaining strong coupling expansions from Hamiltonians with two perturbative terms. The feasibility has indeed been demonstrated, with the following results: errors have been exposed in a previous low-order calculation and corrected series presented, the position of the second-order phase transitions have been confirmed and the behaviour of the line of first-order transitions has been illuminated.

The method is presently being extended in investigations of Z_2 Abelian Higgs in $D=3+1$ and a simple Hamiltonian formulation of QCD with Susskind fermions.

Acknowledgments

I would like to thank the SERC for financial support and Dr A C Irving for technical assistance and advice.

Appendix 1. Series generation of VED from a Hamiltonian with two perturbative terms

Consider the Hamiltonian

$$H = H_0 + \eta H_0' - xV - \xi xV' = H_0 - xV - \xi xV' \tag{A1.1}$$

with the exact eigenvalue equation $H\Psi = E\Psi$, where

$$\Psi = \sum_{r,s=0}^{\infty} \xi^s x^{r+s} \psi_{r+1,s+1} \qquad \psi_{r,s} = \sum_{k,m} \alpha_{rs}(k, m)|km\rangle$$

and

$$E = \sum_{r,s=0}^{\infty} \xi^s x^{r+s} E_{r+1,s+1}.$$

Here $|km\rangle$ are the eigenstates of the unperturbed Hamiltonian and the indices k, m, which label the states, are the eigenvalues of H_0, H_0' respectively. Thus

$$H_0|km\rangle = E(k)|km\rangle \qquad H_0'|km\rangle = E(m)|km\rangle.$$

To simplify the notation and facilitate computation, a matrix notation for the expansion is introduced. Let (m, k) denote an array of coefficients in x and ξx. By working to overall order x^M, attention is restricted to the leading triangle of coefficients

which are limited by the constraint $m+k=M+2$. Thus

$$E_M=\sum_{r=0}^{m}\sum_{s=0}^{k}\xi^s x^{r+s}E_{r+1,s+1}\equiv\begin{array}{c|ccc} & k=1 & 2 & 3\\ m=1 & E_{11} & E_{12} & E_{13}\\ 2 & E_{21} & E_{22} & \cdot\\ 3 & E_{31} & \cdot & \cdot\end{array}.$$

Now

$$\begin{aligned} H&=\tilde{H}_0-xV-\xi xV'\\ (H-E_{11})&=-xV-\xi xV'-(\boldsymbol{E}-E_{11}).\end{aligned}\tag{A1.2}$$

By projecting onto $\langle km|$ and letting

$$\langle km|=\sum_{r,s=0}^{\infty}\alpha_{r+1,s+1}(km)\xi^s x^{r+s}=\boldsymbol{\alpha}(km)$$

(A1.2) becomes

$$\boldsymbol{\alpha}(km)=\frac{(\boldsymbol{E}-E_{11})\boldsymbol{\alpha}(km)-x\,\Sigma_{k'm'}V_{km}^{k'm'}\boldsymbol{\alpha}(k'm')-\xi x\,\Sigma_{k'm'}V_{km}^{\prime k'm'}\boldsymbol{\alpha}(k'm')}{E(km)-E_{11}}.\tag{A1.3}$$

Here $V_{km}^{k'm'}$ are the matrix elements which connect states $|k'm'\rangle$ with $|km\rangle$. Iterative use of (A1.3) enables the generation of higher-order coefficients belonging to the arrays $\boldsymbol{\alpha}$, and thus $|\Psi\rangle$.

The energy estimate obtained (to order M) is

$$\varepsilon_M=\frac{\langle\Psi_M|H|\Psi_M\rangle}{|\Psi_M|^2}=\boldsymbol{E}+\mathrm{O}(x^{2M+2}).\tag{A1.4}$$

One can see that $|\Psi\rangle$ need only be evaluated to order M to obtain an expansion for $\boldsymbol{E}$ to order $2M+1$.

Explicitly, ε_M is evaluated via

$$\varepsilon_M=\frac{\Sigma_{k,m}E(k,m)|\boldsymbol{\alpha}(k,m)|^2-x\,\Sigma_{k'm'}V_{km}^{k'm'}\boldsymbol{\alpha}(km)\boldsymbol{\alpha}(k'm')-\xi x\,\Sigma_{k'm'}V_{km}^{\prime k'm'}\boldsymbol{\alpha}(km)\boldsymbol{\alpha}(k'm')}{\Sigma_{km}|\boldsymbol{\alpha}(km)|^2}.$$

The initial conditions depend upon the unperturbed values of H_0. In the case in question here,

$$\psi_{11}=1\qquad\frac{\langle\Psi_M|H|\Psi_M\rangle}{\langle\Psi_M|\Psi_M\rangle}=0.$$

The calculation of the series for the VED proceeds as follows.

(i) Construction of a (compact) matrix representation for V and V' connecting states on a given cluster (m,α_m).

(ii) Use of the above algorithm to calculate $\omega_{m,\alpha_m}(\boldsymbol{E})$ for all clusters contributing at a given order. The relevant α are evaluated using (A1.3), and are then used in (A1.4) to evaluate $\boldsymbol{E}$, which is then used in turn in (A1.3), etc.

(iii) Inversion of (2.4) to obtain ε_{m,α_m}.

(iv) Multiplication of the ε by the corresponding lattice constants. Subsequent summation yields the VED.

Appendix 2. Series expansion for the mass gaps of a Hamiltonian with two perturbative terms

To produce the required perturbative expansion for Δ_{m,β_m} (2.7), let D_{m,β_m} be the matrix whose lowest eigenvalue is Δ_{m,β_m}; then D_{m,β_m} has the block matrix form (Irving and Hamer 1984a)

$$D_{m,\beta_m} = \left(\begin{array}{c|c} 0 & -\langle 1|x\tilde{V}P \\ \hline -Px\tilde{V}|1\rangle & P(\tilde{H}_0' - x\tilde{V})P \end{array}\right) \tag{A2.1}$$

where $x\tilde{V} = x(V + \xi V')$ and $\tilde{H}_0' = H_0 + \eta H_0' + (\Delta_{m,\beta_m} - F)$. Other notation is as given in the text.

The values of the overall mass gaps F and cluster contributions Δ_{m,β_m} are calculated in an iterative fashion, the algorithm being derived in a similar way to that used in appendix 1.

One obtains

$$\boldsymbol{\alpha}(km) = \frac{(\Delta_{m,\beta_m} - E_{11})\boldsymbol{\alpha}(km) - x\,\Sigma_{k'm'}\, V_{km}^{k'm'}\boldsymbol{\alpha}(km) - \xi x\,\Sigma_{k'm'}\, V_{km}^{\prime k'm'}\boldsymbol{\alpha}(km)}{E_0(km) + (\Delta_{m,\beta_m} - \boldsymbol{F})}. \tag{A2.2}$$

The denominator may be re-expressed as $E_0(km) - E_{11} + (\Delta_\beta - F)^{k,m\geqslant 2}$. Here E_{11} again refers to the unperturbed energy of the first excited state. Now

$$\Delta_{m,\beta_m} = \frac{\langle \Psi_M | D_{m,\beta_m} | \Psi_M \rangle}{|\Psi_M|^2} \tag{A2.3}$$

$$= \Delta_{m,\beta_m} + O(x^{2M+2})$$

$$= \frac{\Sigma_{km}\,(\Delta_{m,\beta} - \boldsymbol{F})|\boldsymbol{\alpha}(km)|^2 - x\,\Sigma_{k'm'}\, V_{km}^{k'm'}\boldsymbol{\alpha}(k,m)\boldsymbol{\alpha}(k'm') - \xi x\,\Sigma_{k'm'}\, V_{km}^{\prime k'm'}\boldsymbol{\alpha}(km)\boldsymbol{\alpha}(k'm')}{\Sigma_{km}\,|\boldsymbol{\alpha}(k,m)|^2}. \tag{A2.4}$$

Evaluation of F proceeds as follows.

(i) Initialisation. Here $\psi_{11} = 1$, $E_{11} = F_0$.

(ii) (A2.2) is used to evaluate the relevant $\boldsymbol{\alpha}$ which are then used in (A2.4) to evaluate Δ_{m,β_m} for a particular cluster.

(iii) Δ_{m,β_m} is calculated for all clusters contributing at a particular order.

(iv) These are then used to obtain an expression for $\boldsymbol{F}$ via (2.6) and (2.7).

(v) $\boldsymbol{F}$ is then used in (A2.2) to evaluate the necessary $\boldsymbol{\alpha}$ to the next highest order.

References

Banks J L and Sinclair D K 1981 *Phys. Rev.* D **23** 2963

Banks T, Raby S, Susskind L, Kogut D R T, Scharbach P N and Sinclair D K 1977 *Phys. Rev.* D **15** 1111

Fradkin E and Shenker S 1979 *Phys. Rev.* D **19** 3682

Fradkin E and Susskind L 1978 *Phys. Rev.* D **17** 2637

Hamer C J 1983 *J. Phys. A: Math. Gen.* **16** 1257

Hamer C J and Irving A C 1985 *Z. Phys.* C **27** 145

Horn D and Karliner M 1982 *Phys. Lett.* **109B** 288

Horn D and Katznelson E 1980 *Phys. Lett.* **91B** 397

Horn D and Yankielwicz S 1979 *Phys. Lett.* **85B** 347

Hornby P G and Barber M N 1985 *J. Phys. A: Math. Gen.* **18** 827

Irving A C and Hamer C J 1984a *J. Phys. A: Math. Gen.* **17** 1649
—— 1984b *Nucl. Phys.* B **230** 336
Irving A C and Thomas A 1982 *Nucl. Phys.* B **200** 424
Kogut J B 1979 *Rev. Mod. Phys.* **51** 659
—— 1980 *Phys. Rev.* D **21** 2316
Marland L G 1981 *J. Phys. A: Math. Gen.* **14** 2047
Nickel B G 1980 unpublished
Pfeuty P and Elliott R J 1971 *J. Phys. C: Solid State Phys.* **4** 2370
Susskind L 1977 *Phys. Rev.* D **16** 3031